Optimizing multi-LGS WFS AO performance in the context of sodium profile evolution and non-common path aberration

Lianqi Wang, Brent Ellerbroek, Glen Herriot, Jean-Pierre Véran, Corinne Boyer

Lianqi Wang, Brent Ellerbroek, Glen Herriot, Jean-Pierre Véran, Corinne Boyer, "Optimizing multi-LGS WFS AO performance in the context of sodium profile evolution and non-common path aberration," Proc. SPIE 10703, Adaptive Optics Systems VI, 107032B (10 July 2018); doi: 10.1117/12.2312873

SPIE.

Event: SPIE Astronomical Telescopes + Instrumentation, 2018, Austin, Texas, United States

Optimizing Multi-LGS WFS AO Performance in the Context of Sodium Profile Evolution and Non-Common Path Aberration

Lianqi Wang[1*], Brent Ellerbroek[2], Glen Herriot[3], Jean-Pierre Véran[3], and Corinne Boyer[1]

[1]Thirty Meter Telescope Project, 100 West Walnut Street Suite 300, Pasadena, CA, 91124, USA

[2]Retired

[3]National Research Council Canada, Victoria BC V9E 2E7, Canada

ABSTRACT

For Extremely Large Telescope (ELT) adaptive optics (AO) systems, multiple Sodium Laser Guide Star (LGS) wavefront sensors (WFSs) are required to achieve high sky coverage and diffraction limited performance. However, temporal and spatial variation of the sodium profile causes measurement biases that appear at all time scales and vary between LGS WFSs. To make things worse, optical design residuals, polishing and alignment errors also create non-common-path aberrations (NCPA) that vary between sub-apertures and different WFS, causing LGS WFS to work significantly off null with a nonlinear response. The induced aberrations are consequently non-radially symmetric, even for center launch laser beams with polar coordinate detectors.

Natural guide star (NGS) based truth wavefront sensors are often suggested as a method of sensing these LGS WFS aberrations, but a single sensor will suffer strong anisoplanatism that may introduce additional errors. In this paper, we present mitigation strategies and performance estimations based on simulations for the Thirty Meter Telescope (TMT) Narrow Field Infrared AO system (NFIRAOS).

1. INTRODUCTION

Sodium laser guide star (LGS) Shack-Hartmann wavefront sensors (WFSs) based adaptive optics (AO) systems have been well established to conquer sky coverage limitation of conventional natural guide star (NGS) WFS based systems. However, in additional to the well known cone effect and tip/tilt uncertainty which have largely been mitigated by using multiple LGS and low order tip/tilt natural guide stars, LGS WFS also suffers measurement uncertainty due to variations in the sodium layer[7] range and profile, which gets progressively worse as the telescope diameter increases. The range variation causes focus measurement error that is significant even at short time scales (~5 Hz) for extremely large telescopes (ELTs). The usual approach is to use slower NGS WFS measurements to update the focus component of the LGS gradients reference vector. For AO systems that employ multiple laser guide stars, however, past lidar measurements[8] have indicated possible significant differences in range between different laser beams, which will no longer have pure focus effect after passing through tomography. To mitigate this effect, we will apply high pass filter (HPF) to the focus mode measurement of each LGS WFS, while simultaneously applying an complementary low pass filter (LPF) on the focus mode measurement of the low order NGS WFS. The frequency split depends on the brightness of the NGS and the variation time scale of such focus measurement error.

The finite thickness of the sodium layer (~10 km) causes elongation of subaperture spot which is approximately proportional to the distance between the subaperture and the laser launch telescope (LLT) and along the baseline between two. As the sodium profile evolves, the elongation pattern changes, which in turn causes gradient measurements biases. For central launch adaptive optics (AO) systems with polar coordinate detector,[2] like the Thirty Meter Telescope (TMT) Narrow Field InfraRed Adaptive Optics System (NFIRAOS), the measurement error is dominated by radially symmetric modes, except non-uniformities arising from off null operation due to non-common-path aberration (NCPA), which includes lenslet to CCD alignment error. A moderately higher order but low speed NGS WFS is consequently necessary to remove such radially symmetric errors. Such a WFS is conveniently named as a truth wavefront sensor (TWFS). We will quantify the residuals after TWFS correction via simulations.

The sodium profile variation together with turbulence profile variation may also cause gain variations in the LGS WFS measurement, which, if not corrected, may cause the non-common-path aberration (NCPA) calibration vectors to be

*Send correspondence to Lianqi Wang (lianqiw@tmt.org)

Adaptive Optics Systems VI, edited by Laird M. Close, Laura Schreiber, Dirk Schmidt, Proc. of SPIE Vol. 10703, 107032B · © 2018 SPIE
CCC code: 0277-786X/18/$18 · doi: 10.1117/12.2312873

incorrectly applied. The actual gain is usually determined by dithering the laser beam at certain pattern using fast steering mirrors (FSMs) with known magnitude (e.g. via FSM local sensor) and compare it against synchronous detection of the dither signal in gradient measurements. The gain variation is of less an issue when many pixels are used to sample the elongated spots.

With different elongation direction and magnitude in different subapertures, the number of illuminated pixels and intensity distribution often vary. The commonly used center of gravity (COG) method suffers in measurement error due to photon and readout noise. Constrained matched filter (CMF) was proposed[5] as a noise optimal solution to mitigate the effects. In this paper, we show that the RMS wavefront error due to noise is significantly reduced by using CMF. However, CMF has its own share of difficulties. Firstly, it requires real time knowledge of the sodium profile in order to compute the CMF. The above mentioned dithering process can be used to derive CMF using measurement data.[10] However, this means that the AO loop have to start with alternative pixel processing algorithm, such as COG, in order start the dithering process. In this way, any non-linearities in COG algorithm not compensated by the TWFS will be affecting the CMF. Secondly, the CMF is a self referencing algorithm and may drift as it is updated using dithering algorithm. In this paper, we show that outer loops to control the drift is essential for stable performance.

Previously, we reported simulation work done in CMF updating.[10] However, realistic off null operation due to NCPA effects were not included in the simulations. Simulations used sodium profile only from a single night. In this paper, we include the effects of NCPA and alignment errors (only on the WFS path, ignored on the science path) , and also multiple sodium profile datasets to quantify the residual over short and long time scales.

The following sections are organized as follows. Section 2 presents the parameters of the TMT AO system NFIRAOS which our modeling is based upon and our simulation parameters. Section 3 reviews the offset and gain calibration. Section 4 and 5 presents the end to end simulation results and performance degradation. Section 6 shows long term stability concerns. Section 7 presents the conclusion.

2. NFIRAOS

The TMT NFIRAOS[6] is an order 60x60 MCAO system with two deformable mirrors (DMs) conjugated to ranges of zero and 11.8 km. Six sodium LGS arranged in a pentagon of 35" radius plus on axis are sensed by LGS Shack-Hartmann WFS. Each LGS WFS uses a polar coordinate detector which has pixel islands from 6x6 to 15x6 arranged radially at the center of each subaperture, with each pixel covering 0.8" on sky to match the projected LGS spot size. This significantly reduces the number of pixels required on the detector to read out and process.

Up to three NGS are picked off by low order on-instrument wavefront sensors sensing in the near infrared. The imaging instrument can optionally provide four on-detector-guide-windows for fast tip/tilt sensing and/or low speed flexure compensation. One pyramid WFS in NFIRAOS is used to provide truth wavefront sensing in LGS AO mode and high order wavefront sensing in classic NGS AO mode. The pyramid WFS has a band pass of 0.61-0.785μm with a nominal order of 96x96 and optional power of 2 binning factors (up to 16).

Our simulations are based upon the full scale model of NFIRAOS, with 7 256x256 meter turbulence layers sampled at 1/64 meter. Each screen is further multiplied by a matching scaling map generated from a spatial PSD to simulate the variation of seeing as measured (and extrapolated) from DIMM/MASS measurement data.[9] The turbulence profile used in simulation is listed in Table 1. A realization of design, polishing, and alignment error of telescope, AO and instrument optics are included. The DM flat and WFS calibration reference vector are computed based upon ray tracing results of these optics.

The nominal signal level per frame for each fully illuminated LGS subaperture is 900 PDE. The read out noise of LGS WFS pixel is 3e. Slodar[11] is used during the simulation to estimate the turbulence profile and update the tomography weighting.[4]

Sodium profiles measured over 33 nights (2009 to 2010) were included in the simulations to collect statistics. Figure 1 shows the averaged sodium profiles of each dataset, with the nominal sodium profile also shown on the last column. The sodium profiles were down sampled to every 10 seconds to reduce measurement noise. The vertical resolution is 200 meters. The profiles are played at 100x the real speed to reduce simulation time, with linear interpolation between sampling points for smooth transitioning. An additional sodium range variation is added to account for higher frequency effects faster than 10 seconds according to the power law.

Altitude (km)	Layer Weighting (r_0=0.186m)	wind speed (m/s)
0	0.4557	5.6
0.5	0.1295	5.8
1	0.0442	6.3
2	0.0506	7.6
4	0.1167	13.3
8	0.0926	19.1
16	0.1107	12.1

Table 1. C_n^2 profile models for the Mauna Kea 13N site. TMT has no direct measurement of the outer scale. We use a conservative value of 30 m.[1]

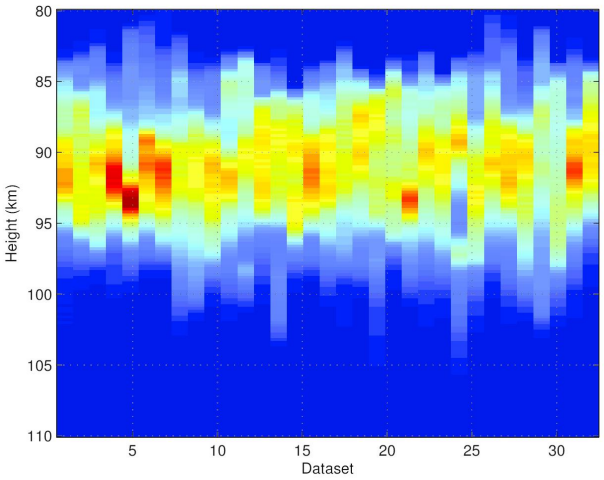

Figure 1. Sodium profiles used in simulations from 33 nights.

The LGS focus error is slowly fixed by a focus mechanism (trombone) shared by all six LGS with an update rate of 0.3 seconds. The trombone is set to null the LGS WFS focus error in the beginning of simulation to simulate the LGS focus acquisition step. The LGS WFS pixel processing starts with center of gravity and switches to CMF when the first estimate is available and then updates the CMF regularly.

3. OFFSET AND GAIN CALIBRATION

The theoretical formulation of LGS offset and gain calibration has been presented in the past[10] and is briefly summarized here. The LGS spot is dithered on sky, completing a circular motion every 4 frames (800 Hz nominally) using fast steering mirror (FSM), which is driven locally at high command rate to obtain smooth circular motion. The FSM reports the FSM position sensor signal to NFIRAOS real time controller (RTC) which uses it to determine the dithering signal amplitude. Gradients calculated by the RTC is compared against the dithering pattern to determine the dithering signal phase using phase locked loop (PLL). For center of gravity, the dithering signal magnitude estimated from gradients is compared against the value computed from the FSM position sensor to adjust the gain. For CMF, the image is correlated against the dithering signal to obtain the derivatives of the averaged subaperture image along x/y directions.

The AO loop starts with COG since no CMF is available that matches the current sodium profile. The RTC computes CMF using statistics collected during the dithering process and switch to it once available, which is then updated regularly (ever 3 to 10 seconds). The wavefront reconstruction is updated in the mean time on account of the updated gradient measurement noise statistics and turbulence conditions (using slodar).

4. TURBULENCE AND NOISE FREE SIMULATIONS

We first carried out simulation without atmospheric turbulence or photon/detector noise to isolate the effect of evolving sodium profiles. In particular, we use these simulations to assess the following effects:

1. Compensation of sodium profile induced aberration with TWFS controlling only radial modes
2. Variability of the compensation residual
3. Frame rate requirement of TWFS
4. Comparing residual error using COG and CMF, as well as bootstrapping CMF using COG.

Thanks to the center launch of LGS[3] and polar coordinate detector,[2] only radially symmetric aberrations resulted from sodium profile variation and needs to be controlled. This is certainly true for an ideal AO system. However, with non-common-path surface aberrations and alignment errors, the LGS WFS has to operation off null (up to 0.8" for NFIRAOS). Non-linearities in the WFS gradient measurements may cause non-radial modes to be present.

Past simulations have been mostly carried out using theoretically derived CMF from the sodium profile used in the simulation. However, in practice, such ideal CMF is not feasible in real system because the sodium profile is not measured in real time. Our plan is to start the AO observations using COG and in the mean time collect statistics via dithering the LGS spot on sky to build CMF. The question to ask is 1) how often do we need to update the CMF on account of the sodium profile evolution, and 2) does this method have any shortfalls.

To answer these questions, we carried out simulations using time evolving sodium profiles as measured by the UBC Lidar.[8] We binned the measurements to 200 meter vertical and 10 second temporal resolution to beat down noise. The simulation uses continuously varying sodium profile at every time step by interpolation, with 100x speed up in time to enable simulation over a wide range of sodium profiles. An additional focus term is introduced at every time step to simulate the range variation that is not captured by the 10 second interval. Two flavors of CMFs are used. The first one is built using theoretical model from the sodium profile at the first time step. Another one is bootstrapped from COG using the dithering process.

Figure 2 shows the performance of COG, and the two flavors of CMF in four different set of sodium profiles. A noise free 30x30 truth WFS outputting only radially symmetric modes are turned on at time step 5000. The COG has biases caused by the sodium profile but is only mildly sensitive to sodium profile evolutions. A TWFS compensates the residual to below 30 nm in three out of the four cases. The CMF built using the first sodium profile gradually decreases in performance as the sodium profile evolves, owing to the increased mismatch, which is again well compensated by the TWFS, with even less residual error than CoG. We believe this is because the CoG has nonlinear effects when operating off null, especially along the azimuthal direction when there are only 6 pixels across. The CMF bootstrapped from COG (switched at around time step 1700) have similar behavior as CMF built with the first sodium profile before TWFs has output, but with residuals similar to the COG after TWFS controls radially symmetric modes. In order words, the CMF boot strapped from COG inherits the nonlinear effects of the CoG and does not perform as good as CMF built using theoretical mode.

Figure 3 left panel shows the cumulative distribution function (CDF) of RMS residual wavefront error after TWFS compensation over 33 different set of sodium profiles. The median uncorrectable errors by the TWFS is ~23 nm for COG and COG to CMF bootstrapping, and is ~10 nm for the theoretical CMF.

Figure 3 right panel shows residual error versus TWFS frame rate (with a control gain of 1). Having a100 second exposure on the TWFS is only slightly worse (by $\lesssim$10 nm in quadrature) than a 6 second exposure for majority of the cases.

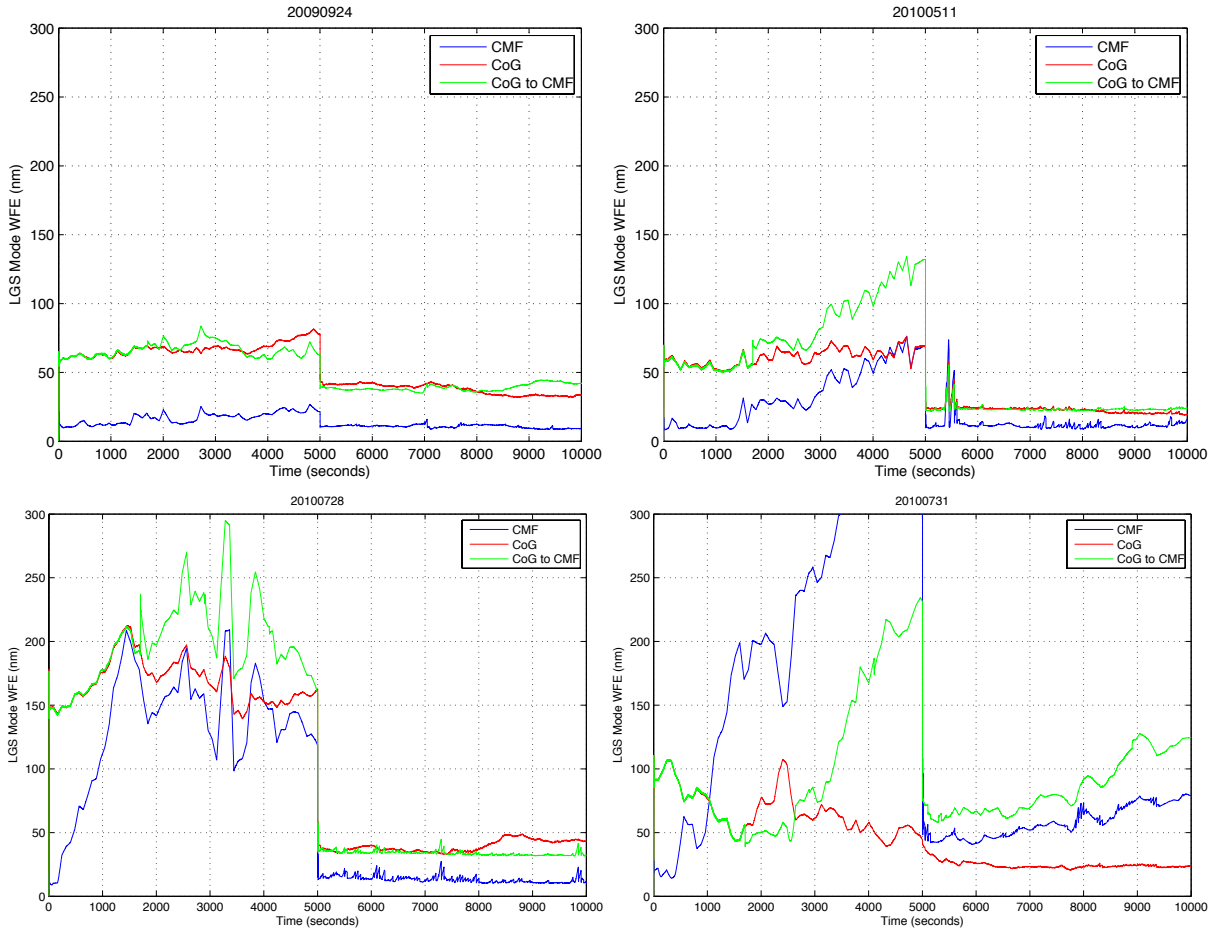

Figure 2. Comparing COG, CMF, and COG to CMF boot strapping. Truth WFS is turned on at frame number 5000.

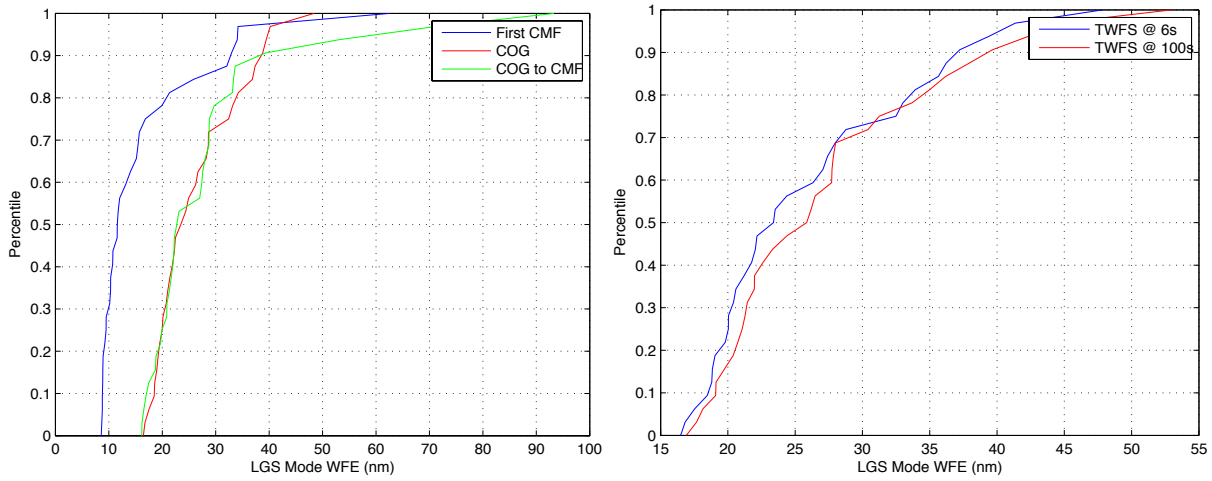

Figure 3. Residual error after TWFS compensation

5. FULL SIMULATIONS

Simulations with turbulence and noise are carried out to assess the performance loss due to sodium profile evolution and noise. The sodium profiles are again accelerated by 100 times to simulate the effects more efficiently. The TWFS has 1 second exposure in the simulation (equivalent to 100 second in actual time) which is sufficient for most cases as demonstrated in 3. Noise is not included in TWFS measurements as this is not the area of concern here. The turbulence uses median seeing conditions at MK13N.[9] The COG uses threshold set to 3 times the read out noise (3 electron).

Figure 4 shows two interesting examples of the performance time history. The top panels show incremental wavefront error (compared against the nominal, static sodium profile, which gives 136.7 nm in noise free and 143 nm in noisy conditions with averaged over two random seeds) for sodium profiles taken at 20100721. The CMF built using the first profile shows steady performance, which indicates weak profile variation, but the COG starts at large error, which indicates large measurement bias due to the profile. The TWFS correcting radially symmetric modes with gain of 1 adequately corrects the error at first shot. Transitioning from COG to CMF improves the performance significantly, especially in the noisy condition. The bottom panels shows results for sodium profiles taken at 20090913. The trend indicates strong profile variation. We plotted the sodium profile for both dates in Figure 5 .

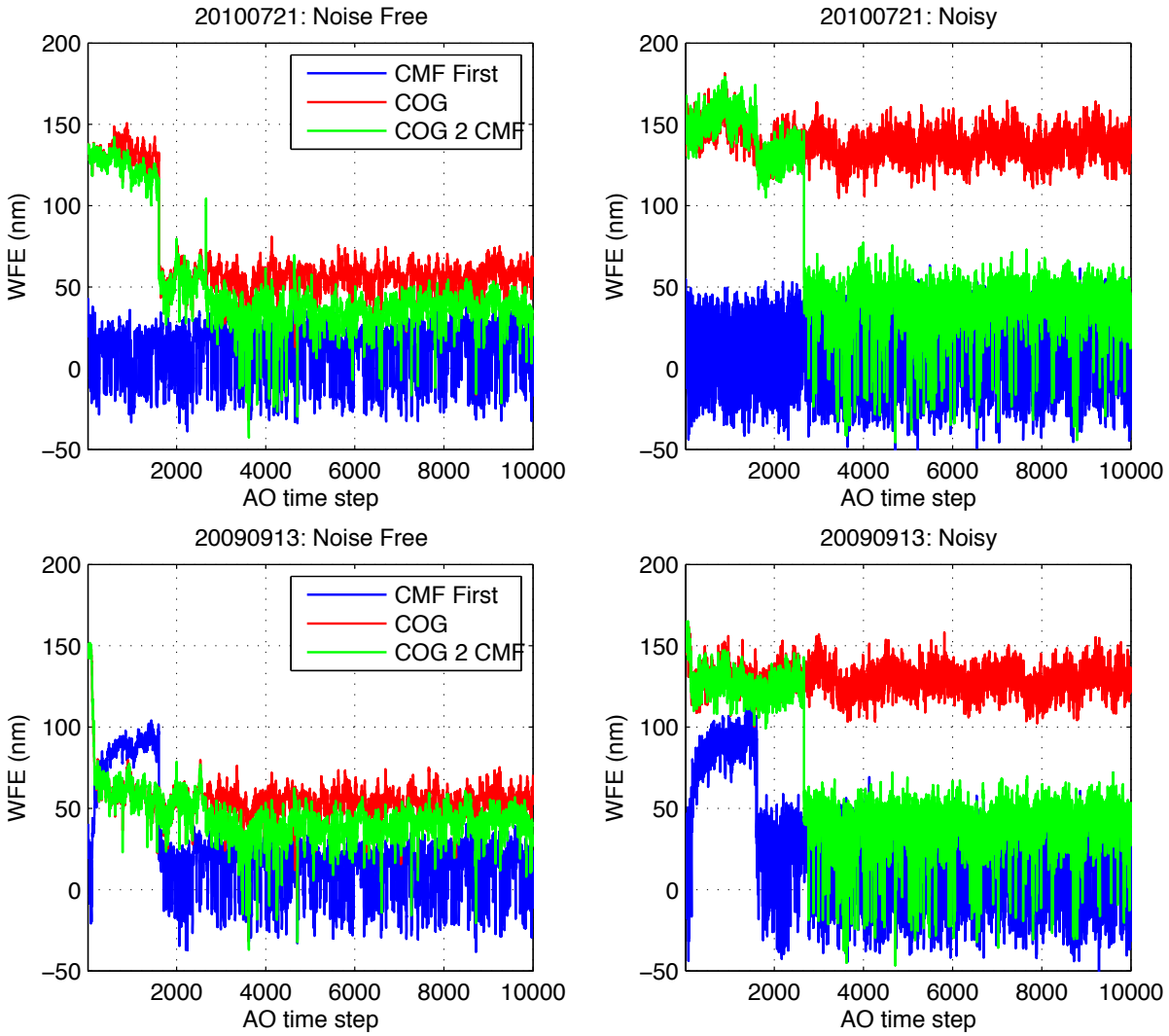

Figure 4. Time history of incremental wavefront error compare against the nominal performance (139 nm noise free, 146 nm noisy). TWFS is turned on at step 1599. COG is switched to CMF at step 2659.

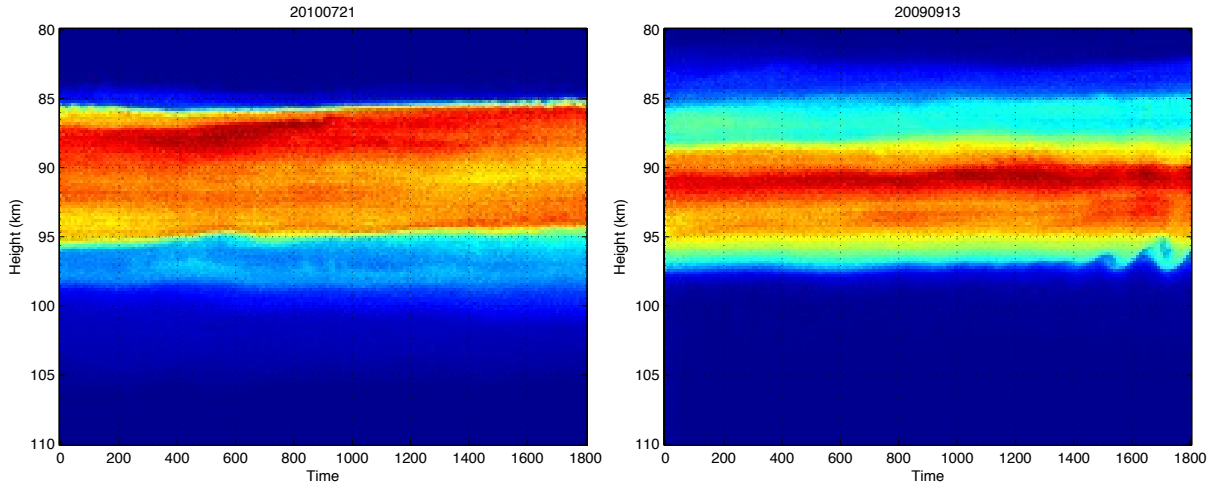

Figure 5. Sodium profiles

Figure 6 shows incremental WFE of time evolving sodium profile compared to nominal sodium profile with each algorithms in noise free (solid) and noisy (dashed) cases. All curves have TWFS correction at 100 second exposure. The performance is evaluated after the CMF gain update is complete.

1. The blue curves labeled as "CMF Mean" is using mean sodium profile in each data set with CMF theoretically computed using the same profile, with no NCPA effect included. The incremental error is within 20 nm in most of the cases, showing that CMF performance is relatively insensitive to the profile shape when build correctly.

2. The red curves labeled as "CMF First" is using ideal CMF theoretically computed with the first sodium profile in the dataset. The performance is close to "CMF Mean", showing that the WFS can correct the profile variation effectively.

3. The green curves labeled as "COG to CMF" starts the AO loop with COG but switch to CMF as soon as it is available via dithering and then updated every 3 seconds. The performance is considerable worse than the first two cases, with 40 nm incremental wavefront error in the median cases.

4. The cyan curves labeled as "COG only" uses COG all the time without any gain update. The noise free performance is not too bad, but the noisy performance is substantially poorer than CMF. The reaffirms the advantage of noise optimal CMF.

5. The magenta curves labeled as "COG Gain Update" uses COG all the time but with its gain updated via dithering. The performance is close to "COG only" case, showing that the gain variation of COG is not significant compared to noise contribution.

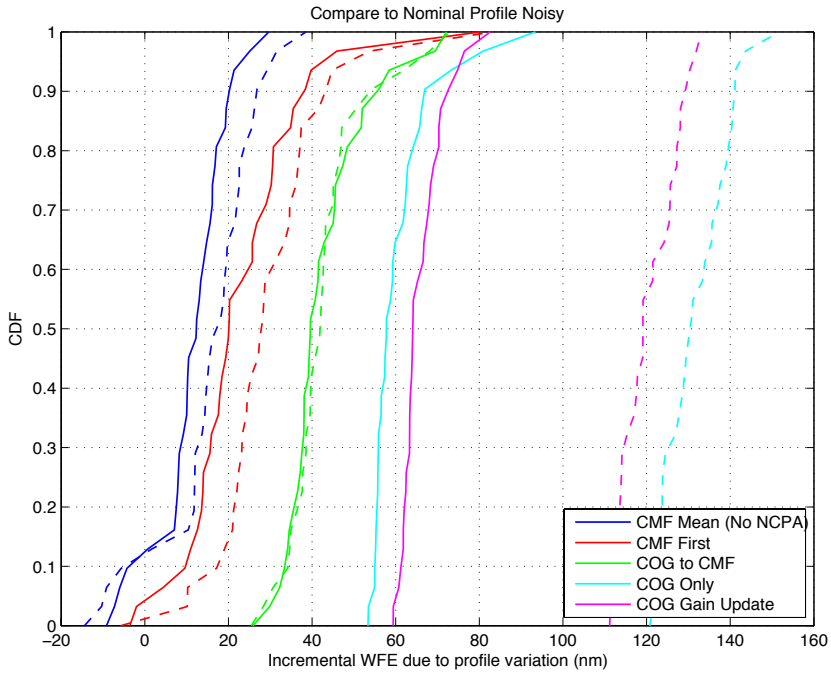

Figure 6. Incremental WFE with evolving sodium profiles compared to nominal sodium profile.

6. LONG TERM STABILITY

For a long observation, the location of the reference image and the phase of the dither signal may drift due to noise and/or numerical error accumulation. This will cause the measured gradient and therefore residual wavefront error to drift if not compensated. The position drift can be estimate by applying COG on the averaged subaperture images, and the phase drift can be estimated by applying COG on the shifted subaperture image using the derivative. Outer loops with low gains can then be constructed to control the gradient reference vector and dither signal phase drift.

Figure 7 shows the incremental wavefront error (compared to nominal sodium profile case) of three 500 second simulations, smoothed to reduce short time variations. The blue curve is with no outer loop, the red curve is with position drift outer loop, and the greed curve is with phase drift outer loop in addition. It is apparent that the position drift outer loop is effective and necessary. However, we didn't observe any phase drift effects during this simulation. The duration may be too short for this effect to be significant.

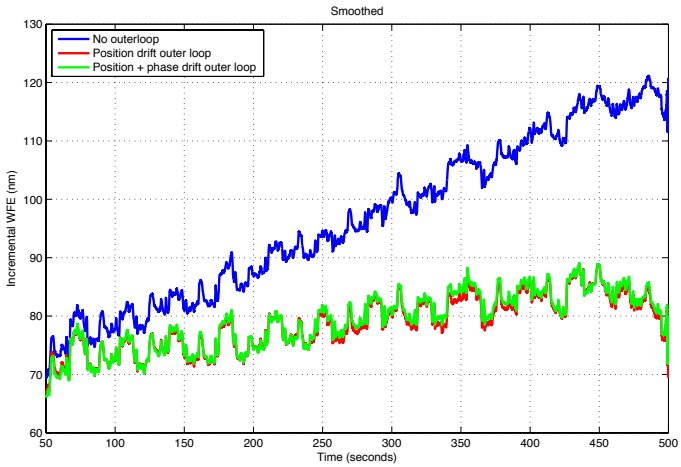

Figure 7. Time history of a long term simulation to show the effect of outer loops. The right panel shows a smoothed version of the left panel.

7. CONCLUSION

We presented simulation results on LGS WFS optimation in the context of sodium profile evolution and NCPA aberration. We show that the boot straping of constrained matched filter and sodium profile variation suffer 40 nm of incremental wavefront error when compared against static nominal profile and ideal constrained matched filter. These results are still preliminary. Further optimization to reduce the incremental error may be possible by, for example, outputting full modes from the TWFS at slower rate.

REFERENCES

[1] A. Abahamid, J. Vernin, Z. Benkhaldoun, A. Jabiri, M. Azouit, and A. Agabi. Seeing, outer scale of optical turbulence, and coherence outer scale at different astronomical sites using instruments on meteorological balloons. *Astronomy and Astrophysics*, 422:1123–1127, August 2004.

[2] Sean Adkins. Measured performance of the prototype polar coordinate ccd array. 2012.

[3] Lianqi Wang Corinne Boyer, Brent Ellerbroek. The tmt laser guide star facility. 2010.

[4] Brent L. Ellerbroek. Efficient computation of minimum-variance wave-front reconstructors with sparse matrix techniques. *J. Opt. Soc. Am. A*, 19(9):1803–1816, 2002.

[5] Luc Gilles and Brent Ellerbroek. Shack-hartmann wavefront sensing with elongated sodium laser beacons: centroiding versus matched filtering. *Appl. Opt.*, 45(25):6568–6576, 2006.

[6] G. Herriot, D. Andersen, J. Atwood, C. Boyer, P. Byrnes, K. Caputa, B. Ellerbroek, L. Gilles, A. Hill, Z. Ljusic, J. Pazder, M. Rosensteiner, M. Smith, P. Spano, K. Szeto, J.-P. Véran, I. Wevers, L. Wang, and R. Wooff. NFIRAOS: first facility AO system for the Thirty Meter Telescope. In *Adaptive Optics Systems IV*, volume 9148 of *Proc. SPIE*, page 914810, July 2014.

[7] G. Herriot, P. Hickson, B. Ellerbroek, J.-P. Véran, C.-Y. She, R. Clare, and D. Looze. Focus errors from tracking sodium layer altitude variations with laser guide star adaptive optics for the Thirty Meter Telescope. In *Society of Photo-Optical Instrumentation Engineers (SPIE) Conference Series*, volume 6272, July 2006.

[8] Thomas Pfrommer and Paul Hickson. High-resolution lidar observations of mesospheric sodium and implications for adaptive optics. *JOSA A*, 27:A95–A105, 2010.

[9] M. Schöck, S. Els, R. Riddle, W. Skidmore, T. Travouillon, R. Blum, E. Bustos, G. Chanan, S. G. Djorgovski, P. Gillett, B. Gregory, J. Nelson, A. Otárola, J. Seguel, J. Vasquez, A. Walker, D. Walker, and L. Wang. Thirty Meter Telescope Site Testing I: Overview. *PASP*, 121:384–395, April 2009.

[10] Lianqi Wang and Brent Ellerbroek. Optimizing lgs wfs pixel processing in the context of evolving turbulence and sodium profile. 2015.

[11] Lianqi Wang, Matthias Schöck, and Gary Chanan. Atmospheric turbulence profiling with slodar using multiple adaptive optics wavefront sensors. *Appl. Opt.*, 47(11):1880–1892, Apr 2008.